中国科学 : 物理学 力学 天文学 2026 年 第 56 卷 第 5 期 : 250003
SCIENTIA SINICA Physica, Mechanica & Astronomica physcn.scichina.com
《中国科学》杂志社 SCIENCE CHINA PRESS
评 述 兰州大学物理学科建立80周年专辑

# 黑洞热力学几何及其微观结构概述

魏少文[1,2*], 刘玉孝[1,2*]

1. 兰州大学兰州理论物理中心, 教育部量子理论与应用重点实验室, 甘肃省理论物理重点实验室, 甘肃省量子物理基础学科研究中心, 兰州 730000
2. 兰州大学物理科学与技术学院, 理论物理研究所, 引力研究中心, 兰州 730000
*联系人, 魏少文, E-mail: weishw@lzu.edu.cn; 刘玉孝, E-mail: liuyx@lzu.edu.cn

收稿日期: 2025-11-04; 接受日期: 2026-01-19; 网络出版日期: 2026-04-13
国家自然科学基金(编号: 12475055, 12475056, 12247101)资助项目

**摘要** 本文重点围绕黑洞热力学相变与微观结构关联, 系统回顾黑洞微观分子模型的研究进展. 首先, 针对小-大黑洞相变问题, 我们详细阐述相变临界点的判定方法及临界现象的特征规律, 为后续模型构建奠定理论基础. 基于相变普适性原理, 提出黑洞微观分子模型的基本框架, 揭示其热力学行为与微观相互作用的潜在联系. 进一步地, 在热力学参数空间中引入Ruppeiner几何, 系统分析该几何结构、线元和标曲率的物理内涵. 通过对比范德瓦尔斯流体与黑洞系统的Ruppeiner几何特征, 深入剖析两者微观结构的异同点, 进而阐明黑洞系统独特的微观相互作用. 基于上述对比分析, 进一步重构了黑洞微观分子间可能的相互作用势能形式, 为理解其非平庸统计行为提供理论支撑. 本文旨在探索黑洞热力学相变与黑洞微观结构之间的内在联系, 通过相变临界现象揭示黑洞的微观结构, 加深对黑洞引力本质的认识.

**关键词** 经典黑洞, 热力学, 相变, 标曲率, 微观结构

**PACS:** 04.70.Dy, 04.60.-m, 05.70.Ce

## 1 引言

黑洞被视为时空区域中引力极强、连光都无法逃逸的天体——当事件视界处的逃逸速度超过光速时, 这种“纯引力”特性似乎使其不具备温度概念, 也不存在熵. 然而, 一个思想实验, 将热茶倒入黑洞会导致茶的熵消失, 违背热力学第二定律, 引发了关键质疑. 为解决这一矛盾, Bekenstein [1,2]提出黑洞具有与事件视界面积直接相关的热力学熵, 尽管Hawking最初对此持怀疑态度, 但后续考虑黑洞视界附近的量子效应后, 他发现黑洞会以特定温度, 即Hawking温度, 向外辐射粒子[3,4]. 由此确立了黑洞熵等于其视界面积1/4的著名结论, 这成为理解黑洞性质的重要里程碑.

此后, Bekenstein [1,2]和Hawking [3,4]的研究被进一步体系化, 形成了黑洞热力学的四大基本定律——该框架成功将强引力系统映射到热力学理论中[5]. 尤其值得注意的是, 量子效应的引入为探究引力理论与热力学之间的深层关联提供了关键路径, 不仅深化了对

引用格式: 魏少文, 刘玉孝. 黑洞热力学几何及其微观结构概述. 中国科学: 物理学 力学 天文学, 2026, 56: 250003
Wei S-W, Liu Y-X. Overview of black hole thermodynamics geometry and its microscopic structure (in Chinese). Sci Sin-Phys Mech Astron, 2026, 56: 250003, doi: 10.1360/SSPMA-2025-0526

© 2026 《中国科学》杂志社 

黑洞本质的认识, 也为理解这两种物理范式的兼容性开辟了重要方向.

作为热力学系统, 相变现象是其核心研究内容之一. 在黑洞热力学理论发展的早期阶段, Hawking和Page [6]在研究反德西特(AdS)空间中的黑洞时, 首次发现纯热辐射相与稳定的大质量黑洞相之间存在一个明确的相变过程, 即著名的Hawking-Page相变. 这一相变现象被后续研究用于解释规范场理论中夸克-胶子等离子体的禁闭与退禁闭相变 [7], 为理解强相互作用系统不同相的行为提供了重要参考. 受AdS/CFT 对应关系的启发 [8–10], AdS空间中的各类相变行为得到了广泛而深入的研究. 特别是在将相关研究拓展至带电黑洞或旋转黑洞体系时, 研究者们发现了自由能随参数变化呈现出的燕尾行为特征. 这种自由能曲线的特殊形态通常暗示着系统在特定参数区间内存在稳定的相变过程或相竞争现象, 为揭示黑洞系统的丰富相结构及其潜在物理机制提供了关键线索 [11–13].

特别地, 2009年, 在文献[14]中提出, AdS空间中的负宇宙学常数可等效为热力学压强, 并由此推导出其对应的热力学第一定律. 基于该理论框架, 研究者发现了与范德瓦尔斯流体气-液相变精确对应的小-大黑洞相变体系, 其临界行为符合平均场理论预言. 这一压强-体积($P$-$V$)临界现象 [15]迅速成为研究热点, 进一步揭示了包括重入相变、三相点、四相点及超流相变等在内的丰富相变结构 [16–31].

在黑洞相变研究取得系列进展的基础上, 如何基于这些宏观现象深入探索黑洞的微观本质, 成为亟待解决的重要科学问题. 众所周知, 宏观相变的本质源于系统内微观组分间相互作用与竞争共存的结果, 因此相变行为能够反映系统的微观特性. 对黑洞而言, 其熵与温度虽可通过引力理论来得到, 但其微观结构仍是待解的核心问题. 尽管现有理论(如弦理论、$D$膜理论、Fuzzball模型等)对此进行了诸多探索 [32–38], 但尚未形成普适且完备的解释. 鉴于热力学相变与微观性质的内在关联, 利用相变现象作为研究黑洞微观结构的切入点, 为该领域提供了全新的研究路径.

首先需明确回答: 黑洞是否具有热力学意义上的微观结构? 从经典引力理论视角看, 黑洞通常被视为高度致密的宏观天体, 而非具有内部微观结构的系统. 但依据玻尔兹曼的朴素热力学观点——“凡可被加热的物体必具有微观结构”, 这一在原子发现前推动物质微观认知的重要思想, 对黑洞同样适用: 黑洞的Hawking温度可通过物质吸收或辐射过程动态改变, 这一特性表明黑洞必然具有某种微观结构, 尽管其具体本质尚未阐明.

热力学几何作为研究系统微观相互作用的有效工具, 通过热力学参数空间中的几何特征(如热容的零点与发散行为)揭示微观相互作用规律 [39–41]. 其中, Ruppeiner几何的标量曲率与流体系统中微观分子间相互作用强度及性质直接相关, 为从热力学视角解析微观结构提供了方法论支持.

基于此, 我们通过构建范德瓦尔斯流体与四维带电AdS黑洞的Ruppeiner几何模型, 系统探索了其微观特性: 研究表明, 范德瓦尔斯流体分子间以吸引相互作用为主导; 而四维带电AdS黑洞除吸引作用外, 还存在显著的排斥相互作用, 这一发现揭示了黑洞区别于经典流体的独特微观结构 [42,43]. 该研究进一步推广至其他黑洞体系, 持续揭示了更多微观结构关联特性. 基于热力学几何所刻画的微观结构特征, 我们进一步重构了黑洞微观分子间可能的相互作用势能形式, 为从热力学角度深入理解黑洞的微观本质提供了理论支撑与新的研究范式.

本文内容安排如下: 第2节系统回顾小-大黑洞相变的研究背景, 重点对相变临界点的判定方法及临界现象的一般特征进行理论分析; 第3节详细阐述黑洞微观分子模型的基本框架与物理内涵, 为后续微观性质研究奠定理论基础; 第4节引入Ruppeiner几何方法, 系统构建热力学参数空间中的几何分析框架, 并深入解析其标量曲率与线元所蕴含的微观相互作用物理信息; 第5节基于Ruppeiner几何的解析结果, 对黑洞系统的微观特性(如分子间相互作用机制与统计行为特征)展开有效讨论; 最后, 第6节总结全文研究进展, 并展望后续研究方向与潜在拓展领域. 文中我们采用如下几何单位制: $G_N = \hbar = c = 1$.

## 2 黑洞相变

在将AdS空间中的负宇宙学常数等效为热力学压强后, 黑洞热力学理论得以拓展至扩展相空间. 研究表明, 小-大黑洞相变与范德瓦尔斯流体中的液-气相变存在深刻类比关系——两者不仅展现出相似的相结构特征, 更呈现出完全一致的临界现象, 如临界指

数标度律. 这一对应关系从宏观层面为黑洞系统可能存在类似微观结构提供了重要理论暗示. 本节将以带电AdS黑洞体系为具体研究对象, 系统回顾该类黑洞相变的物理机制与关键特征, 并通过与范德瓦尔斯流体相变的对比分析, 深入探讨两类系统在相变行为上的共性与差异, 为后续揭示黑洞微观结构的潜在对应关系奠定研究基础.

描述带电AdS黑洞的作用量如下:

$$I=\frac{1}{16\pi}\int_M\sqrt{-g}\left(R-F^2+\frac{6}{l^2}\right). \tag{1}$$

通过作用量变分可得场方程, 进而求解可得黑洞解

$$\mathrm{d}s^2=-f(r)\mathrm{d}t^2+\frac{1}{f(r)}\mathrm{d}r^2+r^2(\mathrm{d}\theta^2+\sin^2\theta\mathrm{d}\phi^2), \tag{2}$$

$$f(r)=1-\frac{2M}{r}+\frac{Q^2}{r^2}+\frac{r^2}{l^2}, \tag{3}$$

其中$M$, $Q$和$l$分别是黑洞的质量、电荷和AdS半径. 利用“Euclidean trick”, 可得黑洞的Hawking温度为

$$T=\frac{f'(r_h)}{4\pi}=\frac{1}{4\pi r_h}\left(1+\frac{3r_h^2}{l^2}-\frac{Q^2}{r_h^2}\right). \tag{4}$$

在广义相对论框架下, 黑洞熵即为Bekenstein-Hawking熵, 为黑洞视界面面积的1/4:

$$S=\frac{A}{4}=\pi r_h^2. \tag{5}$$

无穷远观者测量到视界面上的电势为

$$\Phi=\frac{Q}{r_h}. \tag{6}$$

通过解释, 宇宙学常数或AdS半径可与黑洞体系的压强相对应 [14]

$$P=-\frac{\Lambda}{8\pi}=\frac{3}{8\pi l^2}. \tag{7}$$

简单推导可验证如下黑洞热力学第一定律和Smarr关系成立:

$$\mathrm{d}M=T\mathrm{d}S+\Phi\mathrm{d}Q+V\mathrm{d}P, \tag{8}$$

$$M=2TS+\Phi Q-2PV, \tag{9}$$

其中,

$$V=\frac{4\pi r_{rh}^3}{3} \tag{10}$$

为热力学体积. 通过式(8), 可以发现黑洞质量$M$应该解释成系统的焓而非内能. 从式(4)解出压强

$$P=\frac{T}{2r_h}-\frac{1}{8\pi r_h^2}+\frac{Q^2}{8\pi r_h^4}. \tag{11}$$

将该式与范德瓦尔斯流体的物态方程

$$P=\frac{T}{(v-b)}-\frac{a}{v^2} \tag{12}$$

进行对比, 可发现黑洞系统的比体积可定义为

$$v=2r_h. \tag{13}$$

注意我们已选取了普朗克长度为1. 相应的黑洞系统的物态方程可写为 [15]

$$P=\frac{T}{v}-\frac{1}{2\pi v^2}+\frac{2Q^2}{\pi v^4}. \tag{14}$$

更广泛地, 黑洞的Hawking温度(4)也可以看作是黑洞系统的物态方程. 利用这一物态方程, 我们在图1中画出了黑洞体系的等温线. 当温度低于临界温度$T_c$时, 每条等温线上有两个极值点, 将等温线分成了三段, 依据比体积/视界半径增大的方向, 我们可称其为小黑洞、中黑洞和大黑洞. 通过计算可知, 小黑洞和大黑洞的热容为正, 因此它们是热力学局域稳定的, 而中黑洞温度为负, 其热力学局域不稳定. 随着温度提高, 两个极值点相互靠近, 并且在某个特定温度时, 它们并合为一个, 同时不稳定黑洞模式消失. 超过临界温度$T_c$时, 等温线变成了一条单调递减的曲线. 等温线的这个特定点称为临界点, 它可以通过求解$(\partial_v P)=(\partial_{v,v}P)=0$来确定, 具体值为 [15]

$$T_c=\frac{\sqrt{6}}{18\pi Q},\quad v_c=2\sqrt{6}Q,\quad P_c=\frac{1}{96\pi Q^2}. \tag{15}$$

在约化参数空间下, 各物理量可由其临界值进行约化, 即$\tau=T/T_c$, $p=P/P_c$, $\nu=v/v_c$,

$$p=\frac{8\tau}{3\nu}-\frac{2}{\nu^2}+\frac{1}{3\nu^4}. \tag{16}$$

由此可知, 在约化参数空间下, 物态方程与电荷无关.

相应地, 其Gibbs自由能可通过作用量积分或勒让德变换求出

$$G=M-TS=\frac{r_h}{4}-\frac{2\pi P r_h^3}{3}+\frac{3Q^2}{4r_h}. \tag{17}$$

固定温度下的自由能行为也在图2中给出. 温度较低时, 这里呈现出了一个燕尾行为, 随着温度趋于临界值, 燕尾行为逐渐减小, 并在临界点处消失. 超过临界温度时, 自由能也变为一条单调曲线.

在这两幅图中所呈现的等温线的行为与范德瓦尔斯流体的等温线行为非常相似, 可以断定, 这里也存在类似于液体-气体相变的小黑洞-大黑洞相变. 根据范德瓦尔斯流体知识, 这一相变点可以通过在图1中的等温线上构造等面积率, 或者通过自由能燕尾行为的交叉点来确定(固定温度和压强下, 体系选取自由能最小状态). 需要注意的是, 对黑洞系统而言, 构造其等面积率时, 需将压强表述为热力学体积$V$而非比体积$v$的函数, 否则上述两种方法不等价, 由等面积率得到的相变

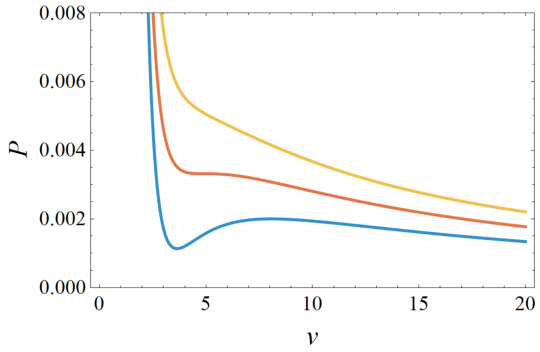


**图 1** 四维带电AdS黑洞的等温线. 温度由下至上依次为$T = 0.8T_c$, $T = T_c$和$T = 1.2T_c$. 电荷$Q = 1$

**Figure 1** The isotherm of a four-dimensional charged AdS black hole. The temperature from bottom to top is $T = 0.8T_c$, $T = T_c$, and $T = 1.2T_c$ with charge $Q = 1$.

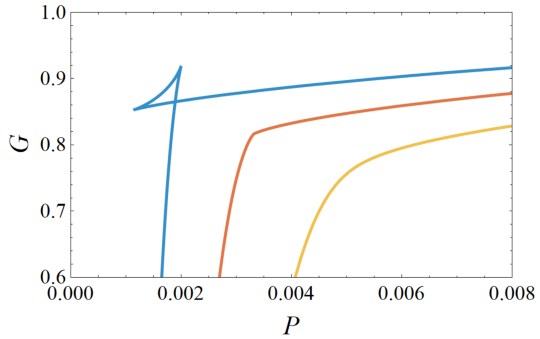


**图 2** 四维带电AdS黑洞的Gibbs自由能. 温度由左至右依次为$T = 0.8T_c$, $T = T_c$和$T = 1.2T_c$. 电荷$Q = 1$

**Figure 2** Behavior of Gibbs free energy of a four-dimensional charged AdS black hole. The temperature from left to right is $T = 0.8T_c$, $T = T_c$, and $T = 1.2T_c$. Charge $Q = 1$.

点也会出现偏差[44].

对四维带电AdS黑洞, 这些相变点构成了一条共存曲线, 具有解析表达形式[45]

$$\tau = \sqrt{\frac{p}{2}}(3 - \sqrt{p}). \tag{18}$$

对于高维带电黑洞, 其解析共存曲线可由下面方法得到. 在相变处, 我们知道大黑洞的视界半径$r_{hl}$总是比小黑洞的视界半径$r_{hs}$大, 因此, 我们可以定义如下参数:

$$\epsilon = 1 - \frac{r_{hs}}{r_{hl}}, \quad \epsilon \in (0,\ 1). \tag{19}$$

进一步借助于等面积率或者燕尾行为, 可以得到共存曲线的解析参数化形式, 但一般来说该形式较为复杂. 对于五维情况, 具体的参数化形式在文献[46]中明确给出.

范德瓦尔斯流体虽然是最早描述这种气-液相变的模型, 但是其共存曲线始终没有解析表达式. 受参数化方法启发, 可定义

$$\epsilon = 1 - \frac{v_l - \frac{1}{3}}{v_g - \frac{1}{3}}, \tag{20}$$

其中$v_g$和$v_l$表示相变点处气体和液体相的约化比体积. 借助于等面积率, 共存曲线的参数化形式为[46]

$$p = \frac{27(1-\epsilon)\left[2\epsilon + (2-\epsilon)\ell_\epsilon\right]^2\left[\epsilon^2 - (1-\epsilon)\ell_\epsilon^2\right]}{\epsilon^2\left[\epsilon + \ell_\epsilon\right]^2\left[\epsilon + (1+\epsilon)\ell_\epsilon\right]^2}, \tag{21}$$

$$\tau = \frac{27\left[(\epsilon-2)\ell_\epsilon - 2\epsilon\right]\left[(2-\epsilon)\epsilon + 2(1-\epsilon)\ell_\epsilon\right]^2}{8\epsilon\left[\epsilon + \ell_\epsilon\right]^2\left[\epsilon - (\epsilon-1)\ell_\epsilon\right]^2}, \tag{22}$$

其中$\ell_\epsilon = \ln(1-\epsilon)$.

除共存曲线外, 另一个值得关注的问题是临界指数. 在临界点处, 借助于$t = 1 - \tau$, 可计算如下4个指数.

(1) 指数$\alpha$刻画定容比热的行为

$$C_v = T\frac{\partial S}{\partial T}\Big|_v \propto |t|^{-\alpha}. \tag{23}$$

(2) 指数$\beta$描述序参量$\eta = v_g - v_l$ (气相体积$v_g$与液相体积$v_l$之差)在给定等温线上的行为

$$\eta = v_g - v_l \propto |t|^{\beta}. \tag{24}$$

(3) 指数$\gamma$决定等温压缩率$\kappa_T$的行为

$$\kappa_T = -\frac{1}{v}\frac{\partial v}{\partial P}\Big|_T \propto |t|^{-\gamma}. \tag{25}$$

(4) 指数$\delta$刻画临界等温线$T = T_c$上的以下关系:

$$|P - P_c| \propto |v - v_c|^{\delta}. \tag{26}$$

通过计算, 这4个临界指数的具体值为

$$\alpha = 0, \quad \beta = \frac{1}{2}, \quad \gamma = 1, \quad \delta = 3. \tag{27}$$

并且它们遵守如下标度率关系

$$\alpha + 2\beta + \gamma = 2, \quad \alpha + \beta(1+\delta) = 2, \tag{28}$$

$$\gamma(1+\delta) = (2-\alpha)(\delta - 1), \quad \gamma = \beta(\delta - 1). \tag{29}$$

这一黑洞相变的研究被推广到了旋转AdS黑洞, 高维AdS黑洞和其他修改引力理论中, 并且发现了包括重入相变、三相点、四相点、超流相等更为丰富的相变类型. 在绝大多数AdS黑洞系统中, 这四个临界指数和标度率均成立, 描述的是一个平均场理论的结果. 但是对于Lovelock和量子反常中的黑洞而言[19,47], 这四个指数在特定临界点为$\alpha = 0, \beta = \frac{1}{2}, \gamma = 1, \delta = 3$. 与一般结果有所差别, 而这一临界点一般称为孤立临界点. 其相结构与普通情况也有所差别.

## 3 黑洞微观分子模型

如第2节所述, 相变现象普遍存在于各类黑洞系统中. 以范德瓦尔斯流体为例, 其气液相变的本质源于微观层面液体分子与气体分子之间的动态竞争与平衡共存过程, 这种微观相互作用可通过经典的刚球模型Lennard-Jones势函数进行精确描述. 类比而言, 黑洞相变行为同样应当源于其构成微观组分间的相互作用与竞争共存机制.

对于范德瓦尔斯流体体系, 其宏观热力学量(如压强、温度等)可通过微观分子结构的统计平均方法严格推导获得; 然而对黑洞系统而言, 尽管其宏观热力学量(如温度、熵等)可借助引力理论的作用量得到, 但其对应的微观结构本质却仍是未解之谜. 这一本质差异恰恰为研究者提供了一个独特而全新的研究视角——从热力学理论出发, 逆向探索黑洞系统的微观结构特征, 进而揭示宏观相变行为与微观机制之间的内在关联.

分子数密度是连接系统宏观与微观性质的重要物理量, 其定义为比体积$v$的倒数, 即[42]

$$n = \frac{1}{v} = \frac{1}{2r_h l_P^2}, \tag{30}$$

这里我们恢复了长度量纲.

从全息的角度来说, 黑洞的热力学是存在于黑洞视界面上. Ruppeiner[40]提出黑洞的每一个微观自由度是由视界面上的每一个普朗克面积元携载的, 如图3所示. 在文献[42], 我们曾提出一个假设, 即一个微观自由度占据$\gamma$个普朗克面积元. 那么, 微观自由度的总数由下式给出:

$$N = \frac{A}{\gamma l_P^2}, \tag{31}$$

于是黑洞的微观分子数密度

$$n = \frac{N}{V} = \frac{3}{\gamma r_h l_P^2}. \tag{32}$$

将其与式(30)进行对比, 可得$\gamma = 6$, 也即黑洞的一个自由度由6个普朗克面积元来描述.

在黑洞经历相变时, 宏观量的变化在一定程度上暗示着黑洞的微观结构进行了突变, 这也可以通过约化的小黑洞和大黑洞分子数密度的$\tilde{n}_s = n_s/n_c$和$\tilde{n}_l = n_l/n_c$来体现

$$\tilde{n}_s = \frac{\sqrt{2}}{2}\left(\sqrt{3 - \sqrt{p}} + \sqrt{3 - 3\sqrt{p}}\right), \tag{33}$$

$$\tilde{n}_l = \frac{\sqrt{2}}{2}\left(\sqrt{3 - \sqrt{p}} - \sqrt{3 - 3\sqrt{p}}\right). \tag{34}$$

在图4中, 我们画出了$\Delta n = \tilde{n}_s - \tilde{n}_l$. 可以明确看到, 温度低于临界值时, $\Delta n$非零, 暗示在经历相变时, 黑洞的微观分子数密度会发生一个突变. 但相变发生在临界点时, 分子数密度及其大小则不会有明显变化. 特别地, 在临界点附近, 我们可以将分子数密度展开如下:

$$\Delta n = 2\sqrt{2}t^{\frac{1}{2}} + \frac{\sqrt{2}}{2}t^{\frac{3}{2}} + O(t^{\frac{5}{2}}). \tag{35}$$

由此可得$\Delta n$的临界指数为1/2.



**图 3** 黑洞微观分子模型, 每一个格子代表一个普朗克面元

**Figure 3** Microscopic molecular model of black hole, where each grid represents a Planck surface area.

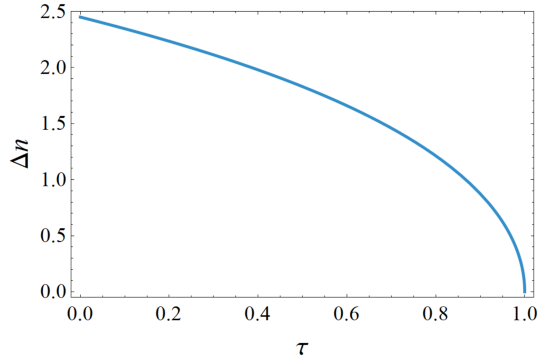


**图 4** 微观分子数密度之差$\Delta n$随温度的变化曲线

**Figure 4** Behavior of number density $\Delta n$ as a function of temperature.

借助于微观分子数密度这一概念, 不同黑洞系统的相关性质得到了详细研究[48–50], 结果表明, 在临界点处, 两相分子数密度之差具有1/2的临界指数, 因此它也可以当作序参量来刻画小-大黑洞相变.

## 4 Ruppeiner几何

热力学几何作为研究黑洞微观结构的重要工具, 主要通过曲率张量等几何量揭示黑洞系统的特殊性质, 特别是热容的零点与发散点等关键热力学特征. 现有研究关注较多的热力学几何方法包括Ruppeiner几何、Weinhold几何等. 本节将重点介绍Ruppeiner几何——该几何框架通过在热力学参数空间中对熵涨落行为进行系统构建, 其理论本质与通过黑洞宏观热力学量反推微观结构的研究思路高度契合, 为从热力学视角探索黑洞微观本质提供了有效方法论支持.

接下来, 我们从统计力学中的玻尔兹曼熵公式出发, 对Ruppeiner几何给出一个简短的引入. 玻尔兹曼熵为

$$S = k_{\mathrm{B}} \ln \Omega, \tag{36}$$

其中玻尔兹曼常数$k_{\mathrm{B}} \approx 1.38 \times 10^{-23}$ J/K. 通过该公式, 热力学系统的微观状态的数目可以表示成

$$\Omega = \mathrm{e}^{\frac{S}{k_{\mathrm{B}}}}, \tag{37}$$

这也是热力学涨落理论的出发点. 对于一个由$N+1$个独立变量$x^{\mu}$组成的系统, 其中$\mu$=0, 1..., $N$, 在$(x^0, ,, x^N)$和$(x^0+\mathrm{d}x^0, , x^N+\mathrm{d}x^N)$之间找到其状态的概率与微状态的数量成正比

$$P(x^0, ..., x^N)\mathrm{d}x^0 \cdots \mathrm{d}x^N = C\Omega(x^0, ..., x^N)\mathrm{d}x^0 \cdots \mathrm{d}x^N, \tag{38}$$

$C$为归一化常数. 那么

$$P(x^0, ..., x^N) \propto \mathrm{e}^{\frac{S}{k_{\mathrm{B}}}}. \tag{39}$$

考虑一个被划分为一个子系统S及其剩余部分的热力学系统, 该子系统被视为环境E. 总熵可以写为$S(x^0, ..., x^N) = S_{\mathrm{S}}(x^0, ..., x^N) + S_{\mathrm{E}}(x^0, ..., x^N)$, 其中$S_{\mathrm{S}} \ll S_{\mathrm{E}} \sim S$. 将总熵在$x^{\mu} = x_0^{\mu}$的局部最大值附近展开, 可得到

$$\begin{aligned} S = S_0 &+ \left.\frac{\partial S_{\mathrm{S}}}{\partial x^{\mu}}\right|_0 \Delta x_{\mathrm{S}}^{\mu} + \left.\frac{\partial S_{\mathrm{E}}}{\partial x^{\mu}}\right|_0 \Delta x_{\mathrm{E}}^{\mu} \\ &+ \frac{1}{2}\left.\frac{\partial^2 S_{\mathrm{S}}}{\partial x^{\mu}\partial x^{\nu}}\right|_0 \Delta x_{\mathrm{S}}^{\mu}\Delta x_{\mathrm{S}}^{\nu} + \frac{1}{2}\left.\frac{\partial^2 S_{\mathrm{E}}}{\partial x^{\mu}\partial x^{\nu}}\right|_0 \Delta x_{\mathrm{E}}^{\mu}\Delta x_{\mathrm{E}}^{\nu} + \cdots, \end{aligned} \tag{40}$$

其中$S_0$为熵的局部最大值, "$|_0$" 表示$|_{x^{\mu}=x_0^{\mu}}$. 很自然地假设涨落参数是保守的和可加的, 即$x_{\mathrm{S}}^{\mu} + x_{\mathrm{E}}^{\mu} = x_{\mathrm{total}}^{\mu}$ =常数; 因此, $\frac{\partial S_{\mathrm{S}}}{\partial x^{\mu}}|_0 \Delta x_{\mathrm{S}}^{\mu} = -\frac{\partial S_{\mathrm{E}}}{\partial x^{\mu}}|_0 \Delta x_{\mathrm{E}}^{\mu}$. 注意到$S_{\mathrm{E}}$与整个系统的熵值大体相同, 则式(40)的最后一项比第四项小得多, 可以忽略. 于是

$$\Delta S = S - S_0 = \frac{1}{2}\left.\frac{\partial^2 S_{\mathrm{S}}}{\partial x^{\mu}\partial x^{\nu}}\right|_0 \Delta x_{\mathrm{S}}^{\mu}\Delta x_{\mathrm{S}}^{\nu} + \cdots. \tag{41}$$

将$S_0$吸收到归一化常数中, 可得以下概率:

$$P(x^0, ..., x^N) \propto \mathrm{e}^{-\frac{1}{2}\Delta l^2}, \tag{42}$$

其中, 两个相邻涨落状态之间的距离线元[40]

$$\Delta l^2 = -\frac{1}{k_{\mathrm{B}}}\frac{\partial^2 S_{\mathrm{S}}}{\partial x^{\mu}\partial x^{\nu}}\Delta x^{\mu}\Delta x^{\nu}. \tag{43}$$

利用黑洞熵, 可得到Ruppeiner几何的有效度规, 同时也可以得到该几何同其他热力学几何间的内在关联. 借助于几何的重要量, 标曲率, 热力学性质得到有效研究, 这一研究方法推广到了各种黑洞背景下并得到了重要结果[51–115].

对于具体的黑洞系统, 利用热力学第一定律, 这一线元可进一步表示为

$$\mathrm{d}l^2 = \frac{C_V}{T^2}\mathrm{d}T^2 - \frac{(\partial_V P)_T}{T}\mathrm{d}V^2. \tag{44}$$

热容$C_V = T(\frac{\partial S}{\partial T})_V$. 基于这一线元公式, 可以类似于黎曼几何一样, 计算它所对应的标曲率$R$, 进而考察系统的相关热力学性质. 在此式及下文中, 我们将取$k_{\mathrm{B}} = 1$.

Ruppeiner几何被广泛应用于不同的流体系统, 通过这些研究获得了以下几个经验总结.

(1) 几何的线元度量两个相邻状态之间的距离. 两个相邻物态之间通过涨落关联的可能性越小, 它们之间的几何线元就越长;

(2) 标曲率的符号可用于考察热力学系统中微观分子之间的相互作用类型. 正、负标曲率分别与排斥和吸引相互作用有关;

(3) 标曲率$R$与热力学系统的关联长度有关: $R \sim \xi^{\bar{d}}$, 其中$\bar{d}$为系统的物理维度;

(4) 标曲率$R$具有临界行为.

## 5 微观结构性质

在这一节中, 我们将介绍如何借助于Ruppeiner几何考察黑洞微观分子间的相关性质.

对于四维带电AdS黑洞, 我们有$S \propto r_h^2$和$V \propto r_h^3$, 这将导致$C_V = 0$. 相应地, 线元(44)会变为退化的, 从而导致标曲率发散. 这一性质对很多带电AdS黑洞都是成立的. 因此利用Ruppeiner几何考察黑洞微观结构的性质似乎是行不通的.

为了解决这一困难, 在文献[43]中, 我们提出了正规标曲率, 其定义为

$$R_{\mathrm{N}} = RC_V. \tag{45}$$

注意到范德瓦尔斯流体的热容量$C_v = \frac{3}{2}k_{\mathrm{B}}$, 其数量级为$10^{-23}$. 因此我们可将黑洞零热容视为$k_{\mathrm{B}} \to 0^+$极限.

对范德瓦尔斯流体, 正规标曲率为[116]

$$R_{\mathrm{N}} = -\frac{2a(v-b)\left(ab + Pv^3\right)}{\left(2ab - av + Pv^3\right)^2}. \tag{46}$$

显然, $R_{\mathrm{N}}$的分母为非负量, 当系统趋近临界点时, 分母趋于0, 从而导致标曲率发散. 对于分子部分, 由于参数$a$和$b$均为正, 当$v \geqslant b$时, $R_{\mathrm{N}} < 0$, 这表明存在吸引相互作用, 与描述范德瓦尔斯流体的刚球模型相符. 此外, 当$a = 0$时, $R_{\mathrm{N}}$为0; 由于$a$衡量分子间相互作用, $a = 0$即表示无相互作用, 这与Ruppeiner几何的经验观测一致. 由于$R_{\mathrm{N}}$的符号与$a$相反, 负(正)曲率标量分别对应吸引(排斥)相互作用. 对于第二项$(v-b)$, 当$b = v$时, 流体系统的所有空间均被微观分子占据, 从而不允许相互作用, 相应的曲率标量亦为0, 这再次与Ruppeiner几何的经验观测相符.

对四维带电AdS黑洞, 其正规标曲率为[43]

$$R_{\mathrm{N}} = \frac{(3\mathcal{V}^{\frac{2}{3}} - 1)(3\mathcal{V}^{\frac{2}{3}} - 4\tau\mathcal{V} - 1)}{2(3\mathcal{V}^{\frac{2}{3}} - 2\tau\mathcal{V} - 1)^2}, \tag{47}$$

其中$\mathcal{V} = V/V_c$为约化热力学体积.

如前所述, 正规标曲率的正负值可揭示系统微观分子之间的相互作用. 为了比较范德瓦尔斯流体和黑洞系统的差别, 我们将具体结果展示在相图图5中. 实线代表气液两相的共存曲线, 虚线代表曲率的符号变化曲线. 区域I具有正标曲率$R$, 表明排斥相互作用在该区域占主导地位. 否则, $R$是负的, 有吸引力的行为占主导地位.

然而, 需要注意的是状态方程在共存线以下不适用, 因此在共存区域中的计算结果是不可靠的, 应该摒弃. 由此, 对于共存线以上的范德瓦尔斯流体, 有吸引力的微观结构相互作用总是占主导地位.

在图6中, 我们描绘了带电AdS黑洞的类似图, 各条曲线所表示的含义与范德瓦尔斯流体类似. 容易看出, 在大$\mathcal{V}$下, 其与范德瓦尔斯流体系统非常相似; 然而, 对于小$\mathcal{V}$来说, 情况明显不同. 除了区域I, 还有两个区域II和III也具有正$R_{\mathrm{N}}$. 与范德瓦尔斯流体一样, 在共存曲线以下, 状态方程不适用, 因此忽略区域I和II. 然而, 共存曲线上方区域III的存在是清晰的. 因此, 在足够高的温度下, 小体积带电AdS黑洞的微观结构之间主要存在排斥相互作用, 这与德瓦尔斯流体的情况形成了鲜明对比. 由于区域III中$R_{\mathrm{N}}$很小, 因此排斥相互作用虽然占主导地位, 但很弱. 在共存曲线上方的其他参数区域, 弱吸引相互作用占主导地位. 通过对不同引力理论中的黑洞进行研究, 除少数系统外, 一般的黑洞均会存在排斥相互作用的情形[43,117–166].

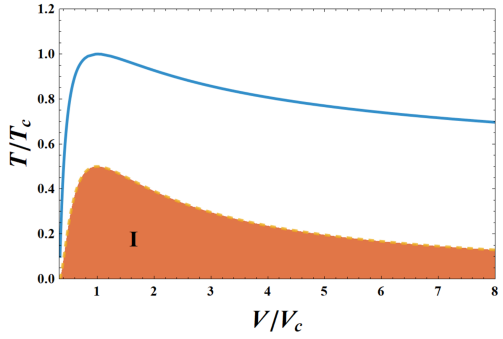


**图 5** 范德瓦尔斯流体的Ruppeiner几何标曲率行为

**Figure 5** The behavior of Ruppeiner geometric curvature for van der Waals fluids.

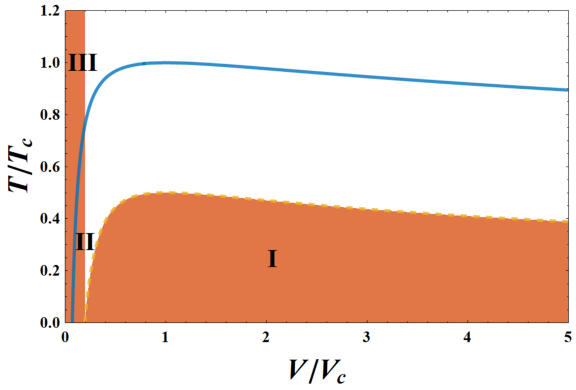


**图 6** 带电AdS黑洞的Ruppeiner几何标曲率行为

**Figure 6** The behavior of Ruppeiner geometric curvature for charged AdS black holes.

如上所示, 尽管状态方程在共存区域不适用, 但$R_{\rm N}$在临界点发散. 接下来, 我们沿着临界点附近的共存小大黑洞曲线研究正规标曲率$R_{\rm N}$的临界行为.

对于四维带电AdS黑洞, 沿着共存小(SBH)和大黑洞(LBH), 在临界点附近展开有如下解析结果:

$$R_{\rm N}({\rm SBH}) = -\frac{1}{8}t^{-2} + \frac{1}{2\sqrt{2}}t^{-\frac{3}{2}} + O(t^{-1}), \tag{48}$$

$$R_{\rm N}({\rm LBH}) = -\frac{1}{8}t^{-2} - \frac{1}{2\sqrt{2}}t^{-\frac{3}{2}} + O(t^{-1}). \tag{49}$$

明显地, 标曲率具有临界指数且为2. 特别地, 由方程(48)和(49), 可得 [43]

$$\lim_{t\to 0} R_{\rm N} t^2 = -\frac{1}{8}. \tag{50}$$

由此, 我们又得到了一个普适常数1/8. 这一结果与范德瓦尔斯流体系统数值结果高度一致. 这一临界行为的研究已经推广到了其他不同黑洞系统, 并且得到了类似结果. 在文献[167]中, 借助于物态方程的解析展开, 临界指数和1/8常数得到了进一步确认.

根据曲率揭示微观分子相互作用的性质, 一个重要的研究是如何重构分子间的势能, 在文献[116]中, 作者进行了初步讨论. 通过定义一个有效电荷

$$q = N \times \frac{Q}{V}, \tag{51}$$

体系物态方程可写为

$$P = \frac{T}{v} - \frac{1}{2\pi v^2}(1 - 4q^2). \tag{52}$$

进一步与范德瓦尔斯流体进行对比, 可得

$$a = \frac{1}{2\pi}(1 - 4q^2), \quad b = 0. \tag{53}$$

前面的研究发现, 带电的AdS黑洞微观结构可以由小黑洞的排斥相互作用主导. 根据Ruppeiner几何的微观解释, 这可以从Lennard-Jones势的角度来理解, 该势在最低点处没有被截断. 存在短程排斥相互作用, 在平均场近似后将导致主导排斥相互作用. 当包含电荷时, 可以精调的方式构造相应的电势. 然而, 正如我们所知, 对于同一状态方程, 分子势并不是唯一的. 在这里, 我们给出一种可能的势形式 [116]

$$\phi = 4\phi_0\left[\left(\frac{r_0}{r + r_0}\right)^{12} - \left(\frac{r_0}{r + r_0}\right)^{6}\right], \tag{54}$$

其中$\phi_0$表示势阱的深度, 参数$r_0$为

$$r_0^3 = \frac{495\left(1 - 4q^2\right)}{248\pi^2\phi_0}. \tag{55}$$

该势能可以给出短程斥力和长程吸引力, 为我们理解黑洞微观结构提供了基础. 其他分子势相关的研究可参见文献[116, 168–172].

## 6 总结和展望

本文系统研究了黑洞热力学相变与微观结构的内在关联, 梳理了黑洞微观分子模型的研究进展, 揭示了其理论框架与物理内涵.

基于相变的一般性研究, 提出了黑洞微观分子模型框架, 明确了热力学行为与微观相互作用之间的潜在联系. 通过引入Ruppeiner几何并深入分析其线元与标曲率的物理意义, 进一步从几何视角阐释了黑洞系统的统计特性. 通过与范德瓦尔斯流体的Ruppeiner几何特征对比, 精准剖析了两者微观结构的异同, 特别是揭示了黑洞系统斥力主导的独特微观相互作用机制. 在此基础上, 重构了黑洞微观分子间可能的相互作用势能形式, 为理解其非平庸统计行为奠定了理论基础.

文章主要讨论了渐近AdS黑洞背景的情形, 对于渐近dS或平直黑洞背景, 这一方法也是可以推广的. 若在这些黑洞系统中存在类似范德瓦尔斯流体的气液相变, 那么微观分子之间将会出现斥力的效应. 若不存在丰富的相变, 而更多地类似于理想气体, 那么这些微观分子间可能就只有引力主导的情形.

综合而言, Bekenstein[1,2]和Hawking[3,4]等人将一个强引力系统映射到了一个热力学系统. 随后, 基于黑洞热力学定律, 相变等宏观热力学行为得到了有效且广泛的研究. 黑洞微观分子模型着眼于从热力学角度考察黑洞的微观结构, 进而希望通过重构的方式对黑洞的引力本质进行探索, 深化我们对强引力的认知.

特别地, 随着黑洞相关的天文观测增加[173], 如何在可观测效应中寻找热力学遗迹, 从而间接证实黑洞热力学也是一个有重要价值的研究方向.

## 参考文献


1 Bekenstein J D. Black holes and the second law. Lett Nuovo Cimento, 1972, 4: 737–740
2 Bekenstein J D. Black holes and entropy. Phys Rev D, 1973, 7: 2333–2346
3 Hawking S W. Black hole explosions? Nature, 1974, 248: 30–31
4 Hawking S W. Particle creation by black holes. Commun Math Phys, 1975, 43: 199–220
5 Bardeen J M, Carter B, Hawking S W. The four laws of black hole mechanics. Commun Math Phys, 1973, 31: 161–170
6 Hawking S W, Page D N. Thermodynamics of black holes in anti-de Sitter space. Commun Math Phys, 1983, 87: 577–588
7 Witten E. Anti-de Sitter space, thermal phase transition, and confinement in gauge theories. Adv Theor Math Phys, 1998, 2: 505–532
8 Maldacena J. The large *N* limit of superconformal field theories and supergravity. Adv Theor Math Phys, 1998, 2: 231–252
9 Gubser S S, Klebanov I R, Polyakov A M. Gauge theory correlators from non-critical string theory. Phys Lett B, 1998, 428: 105–114
10 Witten E. Anti de Sitter space and holography. Adv Theor Math Phys, 1998, 2: 253–291
11 Chamblin A, Emparan R, Johnson C V, et al. Charged AdS black holes and catastrophic holography. Phys Rev D, 1999, 60: 064018
12 Chamblin A, Emparan R, Johnson C V, et al. Holography, thermodynamics, and fluctuations of charged AdS black holes. Phys Rev D, 1999, 60: 104026
13 Niu C, Tian Y, Wu X N. Critical phenomena and thermodynamic geometry of Reissner-Nordström-anti-de Sitter black holes. Phys Rev D, 2012, 85: 024017
14 Kastor D, Ray S, Traschen J. Enthalpy and the mechanics of AdS black holes. Class Quantum Grav, 2009, 26: 195011
15 Kubizňák D, Mann R B. *P-V* criticality of charged AdS black holes. J High Energ Phys, 2012, 2012(7): 033
16 Altamirano N, Kubizňák D, Mann R B. Reentrant phase transitions in rotating anti-de Sitter black holes. Phys Rev D, 2013, 88: 101502
17 Altamirano N, Kubizňák D, Mann R B, et al. Kerr-AdS analogue of triple point and solid/liquid/gas phase transition. Class Quantum Grav, 2014, 31: 042001
18 Altamirano N, Kubizňák D, Mann R, et al. Thermodynamics of rotating black holes and black rings: Phase transitions and thermodynamic volume. Galaxies, 2014, 2: 89–159
19 Dolan B P, Kostouki A, Kubizňák D, et al. Isolated critical point from Lovelock gravity. Class Quantum Grav, 2014, 31: 242001
20 Wei S W, Liu Y X. Critical phenomena and thermodynamic geometry of charged Gauss-Bonnet AdS black holes. Phys Rev D, 2013, 87: 044014
21 Wei S W, Liu Y X. Triple points and phase diagrams in the extended phase space of charged Gauss-Bonnet black holes in AdS space. Phys Rev D, 2014, 90: 044057
22 Frassino A M, Kubizňák D, Mann R B, et al. Multiple reentrant phase transitions and triple points in Lovelock thermodynamics. J High Energ Phys, 2014, 2014(9): 080
23 Cai R G, Cao L M, Li L, et al. *P-V* criticality in the extended phase space of Gauss-Bonnet black holes in AdS space. J High Energ Phys, 2013, 2013(9): 005
24 Xu H, Xu W, Zhao L. Extended phase space thermodynamics for third-order Lovelock black holes in diverse dimensions. Eur Phys J C, 2014, 74: 3074
25 Hennigar R A, Brenna W G, Mann R B. *P-V* criticality in quasitopological gravity. J High Energ Phys, 2015, 2015(7): 077
26 Hennigar R, Mann R. Reentrant phase transitions and van der Waals behaviour for hairy black holes. Entropy, 2015, 17: 8056–8072
27 Hennigar R A, Mann R B, Tjoa E. Superfluid black holes. Phys Rev Lett, 2017, 118: 021301
28 Wu J, Mann R B. Multicritical phase transitions in Lovelock AdS black holes. Phys Rev D, 2023, 107: 084035
29 Wu J, Mann R B. Multicritical phase transitions in multiply rotating black holes. Class Quantum Grav, 2023, 40: 06LT01
30 Kubizňák D, Mann R B, Teo M. Black hole chemistry: Thermodynamics with Lambda. Class Quantum Grav, 2017, 34: 063001
31 Mann R B. Black hole chemistry: The first 15 years. Int J Mod Phys D, 2025, 34: 2542001

32 Strominger A, Vafa C. Microscopic origin of the Bekenstein-Hawking entropy. Phys Lett B, 1996, 379: 99–104
33 Maldacena J M, Strominger A. Statistical entropy of four-dimensional extremal black holes. Phys Rev Lett, 1996, 77: 428–429
34 Callan Jr. C G, Maldacena J M. D-brane approach to black hole quantum mechanics. Nucl Phys B, 1996, 472: 591–608
35 Horowitz G T, Strominger A. Counting states of near-extremal black holes. Phys Rev Lett, 1996, 77: 2368–2371
36 Emparan R, Horowitz G T. Microstates of a neutral black hole in M theory. Phys Rev Lett, 2006, 97: 141601
37 Lunin O, Mathur S D. AdS/CFT duality and the black hole information paradox. Nucl Phys B, 2002, 623: 342–394
38 Lunin O, Mathur S D. Statistical interpretation of the bekenstein entropy for systems with a stretched horizon. Phys Rev Lett, 2002, 88: 211303
39 Weinhold F. Metric geometry of equilibrium thermodynamics. J Chem Phys, 1975, 63: 2479–2483
40 Ruppeiner G. Riemannian geometry in thermodynamic fluctuation theory. Rev Mod Phys, 1995, 67: 605–659 [Erratum: Rev Modern Phys, 1996, 68: 313–313]
41 Liu H, Lü H, Luo M, et al. Thermodynamical metrics and black hole phase transitions. J High Energ Phys, 2010, 2010(12): 054
42 Wei S W, Liu Y X. Insight into the microscopic structure of an AdS black hole from a thermodynamical phase transition. Phys Rev Lett, 2015, 115: 111302 [Erratum: Phys Rev Lett, 2016, 116: 169903]
43 Wei S W, Liu Y X, Mann R B. Repulsive interactions and universal properties of charged anti-de Sitter black hole microstructures. Phys Rev Lett, 2019, 123: 071103
44 Wei S W, Liu Y X. Clapeyron equations and fitting formula of the coexistence curve in the extended phase space of charged AdS black holes. Phys Rev D, 2015, 91: 044018
45 Spallucci E, Smailagic A. Maxwell's equal-area law for charged anti-de Sitter black holes. Phys Lett B, 2013, 723: 436–441
46 Wei S W, Liu Y X. Thermodynamic nature of black holes in coexistence region. Sci China-Phys Mech Astron, 2024, 67: 250412
47 Hu Y P, An Y S, Sun G Y, et al. Quantum anomaly triggers the violation of scaling laws in gravitational system. arXiv: 2410.23783
48 Mo J X, Li G Q. Coexistence curves and molecule number densities of AdS black holes in the reduced parameter space. Phys Rev D, 2015, 92: 024055
49 Wang Y F, Zhang M, Liu W B. Coexistence curve and molecule number density of AdS topological charged black hole in massive gravity. arXiv: 1711.04403
50 Wang Z L, He M, Fang C, et al. The generalization of charged AdS black hole specific volume and number density. Gen Relativ Gravit, 2017, 49: 53
51 Zangeneh M K, Dehyadegari A, Mehdizadeh M R, et al. Thermodynamics, phase transitions and Ruppeiner geometry for Einstein-dilaton-Lifshitz black holes in the presence of Maxwell and Born-Infeld electrodynamics. Eur Phys J C, 2017, 77: 423
52 Gan Q S, Chen J H, Wang Y J. Thermodynamics and geometrothermodynamics of regular black hole with nonlinear electrodynamics. Chin Phys B, 2016, 25: 120401
53 Chaturvedi P, Mondal S, Sengupta G. Thermodynamic geometry of black holes in the canonical ensemble. Phys Rev D, 2018, 98: 086016
54 Wei S W, Liang B, Liu Y X. Critical phenomena and chemical potential of a charged AdS black hole. Phys Rev D, 2017, 96: 124018
55 Zangeneh M K, Dehyadegari A, Sheykhi A, et al. Microscopic origin of black hole reentrant phase transitions. Phys Rev D, 2018, 97: 084054
56 Ruppeiner G. Thermodynamic black holes. Entropy, 2018, 20: 460
57 Eslam Panah B. Effects of energy dependent spacetime on geometrical thermodynamics and heat engine of black holes: Gravity's rainbow. Phys Lett B, 2018, 787: 45–55
58 Yang S J, He Y B, Du J J. The first law and Ruppeiner geometry for Grumiller black hole. Europhys Lett, 2018, 121: 50005
59 Miao Y G, Xu Z M. Parametric phase transition for a Gauss-Bonnet AdS black hole. Phys Rev D, 2018, 98: 084051
60 Zhang M. Corrected thermodynamics and geometrothermodynamics for anti-de Sitter black hole. Nucl Phys B, 2018, 935: 170–182
61 Chen Y, Li H, Zhang S J. Microscopic explanation for black hole phase transitions via Ruppeiner geometry: Two competing factors—The temperature and repulsive interaction among BH molecules. Nucl Phys B, 2019, 948: 114752
62 Ghosh A, Bhamidipati C. Contact geometry and thermodynamics of black holes in AdS spacetimes. Phys Rev D, 2019, 100: 126020
63 Wang P, Wu H, Yang H. Thermodynamic geometry of AdS black holes and black holes in a cavity. Eur Phys J C, 2020, 80: 216
64 Ghosh A, Bhamidipati C. Thermodynamic geometry for charged Gauss-Bonnet black holes in AdS spacetimes. Phys Rev D, 2020, 101: 046005
65 Xu Z M, Wu B, Yang W L. Ruppeiner thermodynamic geometry for the Schwarzschild-AdS black hole. Phys Rev D, 2020, 101: 024018
66 Xu Z M, Wu B, Yang W L. Diagnosis inspired by the thermodynamic geometry for different thermodynamic schemes of the charged BTZ black hole. Eur Phys J C, 2020, 80: 997
67 Singh A, Ghosh A, Bhamidipati C. Thermodynamic curvature of AdS black holes with dark energy. Front Phys, 2021, 9: 631471
68 Xu Z M. The correspondence between thermodynamic curvature and isoperimetric theorem from ultraspinning black hole. Phys Lett B, 2020,

807: 135529
69 Mahish S, Ghosh A, Bhamidipati C. Thermodynamic curvature of the Schwarzschild-AdS black hole and Bose condensation. Phys Lett B, 2020, 811: 135958
70 Wu B, Wang C, Xu Z M, et al. Ruppeiner geometry and thermodynamic phase transition of the black hole in massive gravity. Eur Phys J C, 2021, 81: 626
71 Wei S W, Liu Y X, Mann R B. Novel dual relation and constant in Hawking-Page phase transitions. Phys Rev D, 2020, 102: 104011
72 Mansoori S A H, Rafiee M, Wei S W. Universal criticality of thermodynamic curvatures for charged AdS black holes. Phys Rev D, 2020, 102: 124066
73 Yerra P K, Bhamidipati C. Ruppeiner curvature along a renormalization group flow. Phys Lett B, 2021, 819: 136450
74 Lanteri D, Wan S S, Iorio A, et al. Stability of Schwarzschild (anti)de Sitter black holes in conformal gravity. Eur Phys J C, 2021, 81: 576
75 Castorina P, Lanteri D, Ruggieri M. Fluctuations and thermodynamic geometry of the chiral phase transition. Phys Rev D, 2020, 102: 116022
76 Hu Y P, Cai L, Liang X, et al. Divergence behavior of thermodynamic curvature scalar at critical point in the extended phase space of generic black holes. Phys Lett B, 2021, 822: 136661
77 Pourhassan B, Dehghani M, Faizal M, et al. Non-perturbative quantum corrections to a Born-Infeld black hole and its information geometry. Class Quantum Grav, 2021, 38: 105001
78 Pourhassan B, Wani S S, Soroushfar S, et al. Quantum work and information geometry of a quantum Myers-Perry black hole. J High Energ Phys, 2021, 2021(10): 027
79 Hegde K, Naveena Kumara A, Ajith K M, et al. Thermodynamics, photon sphere and thermodynamic geometry of Ayón-Beato-García Space-time. Int J Mod Phys A, 2025, 40: 2550115
80 Guo S, Liang E W. Ehrenfest's scheme and microstructure for regular-AdS black hole in the extended phase space. Class Quantum Grav, 2021, 38: 125001
81 Gogoi N J, Phukon P. Thermodynamic geometry of 5D *R*-charged black holes in extended thermodynamic space. Phys Rev D, 2021, 103: 126008
82 Wei S W, Liu Y X. General thermodynamic geometry approach for rotating Kerr-anti-de Sitter black holes. Phys Rev D, 2021, 104: 084087
83 Dehyadegari A, Sheykhi A. Thermodynamic geometry and phase transition of spinning AdS black holes. Phys Rev D, 2021, 104: 104066
84 Rafiee M, Hosseini Mansoori S A, Wei S W, et al. Universal criticality of thermodynamic geometry for boundary conformal field theories in gauge/gravity duality. Phys Rev D, 2022, 105: 024058
85 Wang P, Yao F. Thermodynamic geometry of black holes enclosed by a cavity in extended phase space. Nucl Phys B, 2022, 976: 115715
86 Pourhassan B, Aounallah H, Faizal M, et al. Quantum thermodynamics of an M2-M5 brane system. J High Energ Phys, 2022, 2022(5): 030
87 Chaudhary S, Jawad A, Yasir M. Thermodynamic geometry and Joule-Thomson expansion of black holes in modified theories of gravity. Phys Rev D, 2022, 105: 024032
88 Ye X, Chen Z Q, Li M D, et al. QED effects on phase transition and Ruppeiner geometry of Euler-Heisenberg-AdS black holes. Chin Phys C, 2022, 46: 115102
89 Promsiri C, Hirunsirisawat E, Nakarachinda R. Emergent phase, thermodynamic geometry, and criticality of charged black holes from Rényi statistics. Phys Rev D, 2022, 105: 124049
90 Hosseini Mansoori S A, Rafiee M. Criticality of thermodynamic curvatures for D-> 4 consistent Einstein-Gauss-Bonnet black holes. Iran J Phys Res, 2022, 22: 55–69
91 Huang Y, Tao J, Wang P, et al. Phase transitions and thermodynamic geometry of a Kerr-Newman black hole in a cavity. Eur Phys J Plus, 2023, 138: 265
92 Wang C, Wu B, Xu Z M, et al. Thermodynamic geometry of the RN-AdS black hole and non-local observables. Commun Theor Phys, 2024, 76: 025405
93 Xu Z M, Wu B, Yang W L. Rate of the phase transition for a charged anti-de Sitter black hole. Sci China-Phys Mech Astron, 2023, 66: 240411
94 Shahzad M U, Asjad M I, Nafees S, et al. Study of thermodynamical geometries of conformal gravity black hole. Eur Phys J C, 2022, 82: 1044
95 Abdusattar H. Thermodynamic geometry and universal properties of charged anti-de Sitter black hole immersed in perfect fluid dark matter. Phys Dark Univ, 2023, 40: 101228
96 Luciano G G, Sheykhi A. Black hole geometrothermodynamics and critical phenomena: A look from Tsallis entropy-based perspective. Phys Dark Univ, 2023, 42: 101319
97 Xu Z M, Wang Y S, Wu B, et al. Generalized Maxwell equal area law and black holes in complex free energy. Phys Lett B, 2024, 850: 138528
98 Luciano G G, Saridakis E N. *P-V* criticalities, phase transitions and geometrothermodynamics of charged AdS black holes from Kaniadakis

statistics. J High Energ Phys, 2023, 2023(12): 114
99 Chen Z Q, Wei S W. Thermodynamics, Ruppeiner geometry, and topology of Born-Infeld black hole in asymptotic flat spacetime. Nucl Phys B, 2023, 996: 116369
100 Babaei-Aghbolagh H, Mirjalali M, Mahdavian Yekta D, et al. Heat capacities and thermodynamic geometry in deformed Jackiw-Teitelboim gravity. Class Quantum Grav, 2025, 42: 065003
101 Saavedra J F, Tello-Ortiz F. Thermodynamic aspects of FLRW universe in Einstein-Gauss-Bonnet domains. Prog Theor Exp Phys, 2025, 2025(5): 053E01
102 Murgana F, Greco V, Ruggieri M, et al. Functional renormalization group study of thermodynamic geometry around the phase transition of quantum chromodynamics. Phys Rev D, 2024, 109: 096017
103 Singh A. Thermodynamic geometry of dyonic black holes in AdS in extended phase space. Mod Phys Lett A, 2023, 38: 2350173
104 Ghaffari S, Luciano G G, Sheykhi A. Nonextensive entropies impact onto thermodynamics and phase structure of Kerr-Newman black holes. Phys Dark Univ, 2024, 44: 101447
105 Zhang M Y, Chen H, Hassanabad H, et al. Critical behavior and Joule-Thomson expansion of charged AdS black holes surrounded by exotic fluid with modified Chaplygin equation of state. Chin Phys C, 2024, 48: 065101
106 Mann R B. Recent developments in holographic black hole chemistry. J Hologr Appl Phys, 2024, 4: 1–26
107 Sekhmani Y, Luciano G G, Rayimbaev J, et al. Topological AdS black holes surrounded by Chaplygin dark fluid: From stability to geometrothermodynamic analysis. Phys Dark Univ, 2024, 46: 101567
108 Cui H M, Fan Z Y. Criticality of global monopole charges in diverse dimensions. Eur Phys J C, 2024, 84: 1096
109 Ghaffari S, Luciano G G. Black hole thermodynamics in Harada's inspired theory of gravity: Stability, phase structure and geometrothermodynamics. Eur Phys J C, 2025, 85: 785
110 Anand A, Gashti S N, Singh A. Thermodynamic curvature and topological insights of Hayward black holes with string fluids. Phys Dark Univ, 2025, 49: 101994
111 Kruglov S I. Thermodynamic geometry of black holes in AdS space with nonlinear electrodynamics. J Subatom Part Cosmol, 2025, 4: 100101
112 Anand A, Singh A, Mishra A, et al. Black holes in Lorentz-violating gravity: Thermodynamics, geometry, and particle dynamics. Phys Dark Univ, 2025, 50: 102086
113 Ladino J M, Romero-Figueroa C E, Quevedo H. Phase transitions, shadows, and microstructure of Reissner-Nordström-anti-de-Sitter black holes from a geometrothermodynamic perspective. Nucl Phys B, 2024, 1009: 116734
114 Barzi F, El Moumni H, Masmar K. On Rényi microstructural aspects of asymptotically flat charged black holes: A novel duality. Nucl Phys B, 2026, 1022: 117239
115 Abdusattar H. *P-V* criticality and microstructure of hayward black holes in anti-de sitter space. arXiv: 2510.11319
116 Wei S W, Liu Y X, Mann R B. Characteristic interaction potential of black hole molecules from the microscopic interpretation of Ruppeiner geometry. arXiv: 2108.07655
117 Dehyadegari A, Sheykhi A, Montakhab A. Critical behavior and microscopic structure of charged AdS black holes via an alternative phase space. Phys Lett B, 2017, 768: 235–240
118 Chabab M, El Moumni H, Iraoui S, et al. More insight into microscopic properties of RN-AdS black hole surrounded by quintessence via an alternative extended phase space. Int J Geom Methods Mod Phys, 2018, 15: 1850171
119 Miao Y G, Xu Z M. Microscopic structures and thermal stability of black holes conformally coupled to scalar fields in five dimensions. Nucl Phys B, 2019, 942: 205–220
120 Li D, Li S, Mi L Q, et al. Insight into black hole phase transition from parametric solutions. Phys Rev D, 2017, 96: 124015
121 Sun D Q, Deng J B, Li P, et al. Insight into the microscopic structure of an AdS black hole from the quantization. Class Quantum Grav, 2020, 37: 015008
122 Guo X Y, Li H F, Zhang L C, et al. Microstructure and continuous phase transition of a Reissner-Nordstrom-AdS black hole. Phys Rev D, 2019, 100: 064036
123 Wei S W, Liu Y X, Mann R B. Ruppeiner geometry, phase transitions, and the microstructure of charged AdS black holes. Phys Rev D, 2019, 100: 124033
124 Sheykhi A, Arab M, Dayyani Z, et al. Alternative approach towards critical behavior and microscopic structure of the higher dimensional Power-Maxwell black holes. Phys Rev D, 2020, 101: 064019
125 Xu Z M, Wu B, Yang W L. Fine micro-thermal structures for Reissner-Nordström black hole. Chin Phys C, 2020, 44: 095106
126 Wei S W, Liu Y X. Intriguing microstructures of five-dimensional neutral Gauss-Bonnet AdS black hole. Phys Lett B, 2020, 803: 135287

127 Guo X Y, Li H F, Zhang L C, et al. Continuous phase transition and microstructure of charged AdS black hole with quintessence. Eur Phys J C, 2020, 80: 168

128 Ghosh A, Bhamidipati C. Thermodynamic geometry and interacting microstructures of BTZ black holes. Phys Rev D, 2020, 101: 106007

129 Wei S W, Liu Y X. New insights into thermodynamics and microstructure of AdS black holes. Sci Bull, 2020, 65: 259–261

130 Naveena Kumara A, Ahmed Rizwan C L, Hegde K, et al. Microstructure and continuous phase transition of a regular Hayward black hole in anti-de Sitter spacetime. Prog Theor Exp Phys, 2021, 2021(7): 073E01

131 Kumara A N, Rizwan C L A, Hegde K, et al. Repulsive interactions in the microstructure of regular Hayward black hole in anti-de Sitter spacetime. Phys Lett B, 2020, 807: 135556

132 Wei S W, Liu Y X. Extended thermodynamics and microstructures of four-dimensional charged Gauss-Bonnet black hole in AdS space. Phys Rev D, 2020, 101: 104018

133 Xu Z M, Wu B, Yang T, et al. A new measure of thermal micro-behavior for the AdS black hole. Chin Phys C, 2021, 45: 015106

134 Yerra P K, Bhamidipati C. Ruppeiner geometry, phase transitions and microstructures of black holes in massive gravity. Int J Mod Phys A, 2020, 35: 2050120

135 Dehyadegari A, Sheykhi A, Wei S W. Microstructure of charged AdS black hole via *P-V* criticality. Phys Rev D, 2020, 102: 104013

136 Kumara A N, Rizwan C L A, Hegde K, et al. Microstructure of five-dimensional neutral Gauss-Bonnet black hole in anti-de Sitter spacetime via *P-V* criticality. Gen Relativ Gravit, 2023, 55: 4

137 Naveena Kumara A, Ahmed Rizwan C L, Hegde K, et al. Ruppeiner geometry, reentrant phase transition, and microstructure of Born-Infeld AdS black hole. Phys Rev D, 2021, 103: 044025

138 Rizwan C L A, Kumara A N, Hegde K, et al. Coexistent physics and microstructure of the regular Bardeen black hole in anti-de Sitter spacetime. Ann Phys, 2020, 422: 168320

139 Zhou R, Liu Y X, Wei S W. Phase transition and microstructures of five-dimensional charged Gauss-Bonnet-AdS black holes in the grand canonical ensemble. Phys Rev D, 2020, 102: 124015

140 Xu Z M, Wu B, Yang W L. Thermodynamics curvature in phase transitions for AdS black hole. Phys Lett B, 2021, 821: 136632

141 Xu Z M. Analytic phase structures and thermodynamic curvature for the charged AdS black hole in alternative phase space. Front Phys, 2021, 16: 24502

142 Li R, Zhang K, Wang J. Probing black hole microstructure with the kinetic turnover of phase transition. Phys Rev D, 2021, 104: 084076

143 Wei S W, Liu Y X. Testing the microstructure of *d*-dimensional charged Gauss-Bonnet anti-de Sitter black holes. Phys Rev D, 2021, 104: 024062

144 Wei S W, Liu Y X. The microstructure and Ruppeiner geometry of charged anti-de Sitter black holes in Gauss-Bonnet gravity: From the critical point to the triple point. Commun Theor Phys, 2022, 74: 095402

145 Liu F, Du Y Z, Zhao R, et al. Phase equilibrium and microstructure of topological AdS black holes in massive gravity. Chin Phys C, 2022, 46: 085102

146 Aounallah H, El Moumni H, Khalloufi J, et al. Insight into the microscopic structure of a quintessential black hole from the quantization concept. Int J Mod Phys A, 2022, 37: 2250036

147 Bai N, He A, Tao J. Microstructure of charged AdS black hole with minimal length effects. Chin Phys C, 2022, 46: 125105

148 Liu C, Wang J. The radial distribution function reveals the underlying mesostructure of the AdS black hole. J High Energ Phys, 2022, 2022(10): 171

149 Li G R, Li G P, Guo S. Phase transition grade and microstructure of AdS black holes in massive gravity. Class Quantum Grav, 2022, 39: 195011

150 Safir T K, Rizwan C L A, Vaid D. Ruppeiner geometry, *P-V* criticality and interacting microstructures of black holes in dRGT massive gravity. Int J Mod Phys A, 2022, 37: 2250158

151 Ghosh A, Bhamidipati C. Contact and metric structures in black hole chemistry. Front Phys, 2023, 11: 1132712

152 Yu Q, Xu Q, Tao J. Thermodynamics and microstructures of Euler-Heisenberg black hole in a cavity. Commun Theor Phys, 2023, 75: 095402

153 Masood A S Bukhari S, Pourhassan B, Aounallah H, et al. On the microstructure of higher-dimensional Reissner-Nordström black holes in quantum regime. Class Quantum Grav, 2023, 40: 225007

154 Chen D, Tao J, Yang X. Attractive interactions in the microstructures of asymptotically flat black holes. Phys Dark Univ, 2023, 42: 101379

155 Sekhmani Y, Gogoi D J, Myrzakulov R, et al. Phase structures and critical behavior of rational non-linear electrodynamics anti de Sitter black holes in Rastall gravity. Commun Theor Phys, 2024, 76: 045403

156 Feng Z W, Li S Y, Zhou X, et al. Phase transitions, critical behavior and microstructure of the FRW universe in the framework of higher order GUP. Phys Dark Univ, 2024, 46: 101719

157 Beissen N. Geometrothermodynamics of 3D regular black holes. Entropy, 2024, 26: 457
158 Abdusattar H. Beyond classical thermodynamics: Insight into the microstructures of black holes with quantum-triggered violations. arXiv: 2411.13435
159 Deng G M, Huang Y C. $Q$-$\Phi$ criticality and microstructure of charged AdS black holes in $f(R)$ gravity. Int J Mod Phys A, 2017, 32: 1750204
160 Xiao Y. Microscopic derivation of the Bekenstein-Hawking entropy for Schwarzschild black holes. Phys Rev D, 2020, 101: 046020
161 Cai X C, Miao Y G. Can shadows connect black hole microstructures? arXiv: 2101.10780
162 Cai X C, Miao Y G. Connections between entropy surface density and microscopic property in black holes. arXiv: 2103.06667
163 Abdusattar H. Insight into the microstructure of FRW universe from a $P$-$V$ phase transition. J High Energ Phys, 2023, 2023(9): 147
164 Sekhmani Y, Rayimbaev J, Luciano G G, et al. Phase structure of charged AdS black holes surrounded by exotic fluid with modified Chaplygin equation of state. Eur Phys J C, 2024, 84: 227
165 Housset J, Saavedra J F, Tello-Ortiz F. Cosmological FLRW phase transitions and micro-structure under Kaniadakis statistics. Phys Lett B, 2024, 853: 138686
166 Singh A, Mahish S. Criticality of charged AdS black holes with string clouds in boundary conformal field theory. arXiv: 2504.20486
167 Hu Y P, Cai L, Liang X, et al. Divergence behavior of thermodynamic curvature scalar at critical point in the extended phase space of generic black holes. Phys Lett B, 2021, 822: 136661
168 Miao Y G, Xu Z M. Thermal molecular potential among micromolecules in charged AdS black holes. Phys Rev D, 2018, 98: 044001
169 Vargas A F, Contreras E, Bargueño P. SAdS black holes and spacetime atoms: A heuristic approach. Gen Relativ Gravit, 2018, 50: 117
170 Miao Y G, Xu Z M. Interaction potential and thermo-correction to the equation of state for thermally stable Schwarzschild anti-de Sitter black holes. Sci China-Phys Mech Astron, 2019, 62: 10412
171 Dutta S, Punia G S. Interactions between AdS black hole molecules. Phys Rev D, 2021, 104: 126009
172 Xu Z M. Fokker-Planck equation for black holes in thermal potential. Phys Rev D, 2021, 104: 104022
173 Abac A G, Abouelfettouh I, Acernese F, et al. GW250114: Testing Hawking's area law and the Kerr nature of black holes. Phys Rev Lett, 2025, 135: 111403

# Overview of black hole thermodynamics geometry and its microscopic structure

WEI Shao-Wen[1,2*] & LIU Yu-Xiao[1,2*]

[1]*Lanzhou Center for Theoretical Physics, Key Laboratory of Quantum Theory and Applications of MoE, Key Laboratory of Theoretical Physics of Gansu Province, and Gansu Provincial Research Center for Basic Disciplines of Quantum Physics, Lanzhou University, Lanzhou 730000, China*
[2]*School of Physical Science and Technology, Institute of Theoretical Physics & Research Center of Gravitation, Lanzhou University, Lanzhou 730000, China*
**Corresponding authors (WEI Shao-Wen, email: weishw@lzu.edu.cn; LIU Yu-Xiao, email: liuyx@lzu.edu.cn)*

This paper presents a systematic review of research advancements on the microscopic molecular model of black holes, with a central focus on elucidating the intrinsic connection between black hole thermodynamic phase transitions and their underlying microscopic structures. By integrating thermodynamic principles with statistical mechanical frameworks, the study aims to bridge macroscopic observations with microscopic interactions, offering insights into the fundamental nature of black hole gravity. The discussion begins with an in-depth analysis of the small-large black hole phase transition. We detail the rigorous methodologies for identifying critical points and characterizing the associated critical phenomena, such as power-law scaling of thermodynamic quantities near the transition. These results serve as the foundational basis for constructing a microscopic model that can quantitatively reproduce macroscopic phase transitions. Building on the universality principles of phase transitions, we propose a foundational framework for the microscopic molecular model of black holes. This model posits that black hole thermodynamics may emerge from the statistical behavior of hypothetical "microscopic constituents" analogous to molecules in a fluid, with their interactions dictating macroscopic observables. To further explore this connection, we introduce Ruppeiner geometry within the thermodynamic parameter space, analyzing both its line element and scalar curvature. A critical comparative analysis is then conducted between the Ruppeiner geometries of black holes and the classical van der Waals fluid. While both systems exhibit phase transitions, their geometric features diverge significantly: the black hole system demonstrates unique curvature signatures indicative of repulsive interactions. These differences highlight the specialized microscopic structure of black holes, driven by their inherently gravitational nature. Guided by these insights, we reconstruct plausible forms of the interaction potential between black hole microscopic constituents, accounting for the nontrivial statistical behaviors revealed by the geometric analysis. Ultimately, this work synthesizes the logical pathway from phase transition phenomena to microscopic model construction. By doing so, it advances our understanding of the gravitational nature of black holes.

**classical black hole, thermodynamics, phase transition, scalar curvature, microstructure**

**PACS:** 04.70.Dy, 04.60.-m, 05.70.Ce

**doi:** 10.1360/SSPMA-2025-0526